LETTER

doi:10.1038/nature10711

Direct frequency comb spectroscopy in the extreme ultraviolet

Arman Cingöz[1]*, Dylan C. Yost[1]*, Thomas K. Allison[1], Axel Ruehl[2]†, Martin E. Fermann[2], Ingmar Hartl[2] & Jun Ye[1]

The development of the optical frequency comb (a spectrum consisting of a series of evenly spaced lines) has revolutionized metrology and precision spectroscopy owing to its ability to provide a precise and direct link between microwave and optical frequencies[1,2]. A further advance in frequency comb technology is the generation of frequency combs in the extreme-ultraviolet spectral range by means of high-harmonic generation in a femtosecond enhancement cavity[3,4]. Until now, combs produced by this method have lacked sufficient power for applications, a drawback that has also hampered efforts to observe phase coherence of the high-repetition-rate pulse train produced by high-harmonic generation, which is an extremely nonlinear process. Here we report the generation of extreme-ultraviolet frequency combs, reaching wavelengths of 40 nanometres, by coupling a high-power near-infrared frequency comb[5] to a robust femtosecond enhancement cavity. These combs are powerful enough for us to observe single-photon spectroscopy signals for both an argon transition at 82 nanometres and a neon transition at 63 nanometres, thus confirming the combs' coherence in the extreme ultraviolet. The absolute frequency of the argon transition has been determined by direct frequency comb spectroscopy. The resolved ten-megahertz linewidth of the transition, which is limited by the temperature of the argon atoms, is unprecedented in this spectral region and places a stringent upper limit on the linewidth of individual comb teeth. Owing to the lack of continuous-wave lasers, extreme-ultraviolet frequency combs are at present the only promising route to extending ultrahigh-precision spectroscopy to the spectral region below 100 nanometres. At such wavelengths there is a wide range of applications, including the spectroscopy of electronic transitions in molecules[6], experimental tests of bound-state and many-body quantum electrodynamics in singly ionized helium and neutral helium[7–9], the development of next-generation 'nuclear' clocks[10–12] and searches for variation of fundamental constants[13] using the enhanced sensitivity of highly charged ions[14].

Techniques developed to control a train of ultrashort pulses in the frequency domain have led to rapid advancements not only in ultrahigh-precision metrology[1] but also in the generation of attosecond pulses for time-resolved studies[15]. This close relationship between time and frequency techniques continues with the development of the extreme-ultraviolet (XUV) frequency combs, in which high-harmonic generation (HHG), a standard technique in attosecond physics, is used to produce phase-coherent XUV radiation. In conventional HHG, a single infrared pulse generates a burst of attosecond pulses separated by half cycles of the driving laser field, resulting in an odd-harmonic spectrum (Fig. 1). By contrast, in intracavity HHG, a phase-coherent infrared pulse train is used to produce a train of such bursts that repeat at the repetition frequency of the fundamental comb. This new temporal structure is responsible for the much finer frequency comb at each harmonic order. We anticipate that the XUV frequency comb will allow high-precision characterization of the HHG process and provide further insights into attosecond physics.

The existence of the XUV comb structure is critically dependent on the phase coherence of the HHG process. The temporal coherence of HHG in an isolated pulse has been studied extensively[16,17], but the

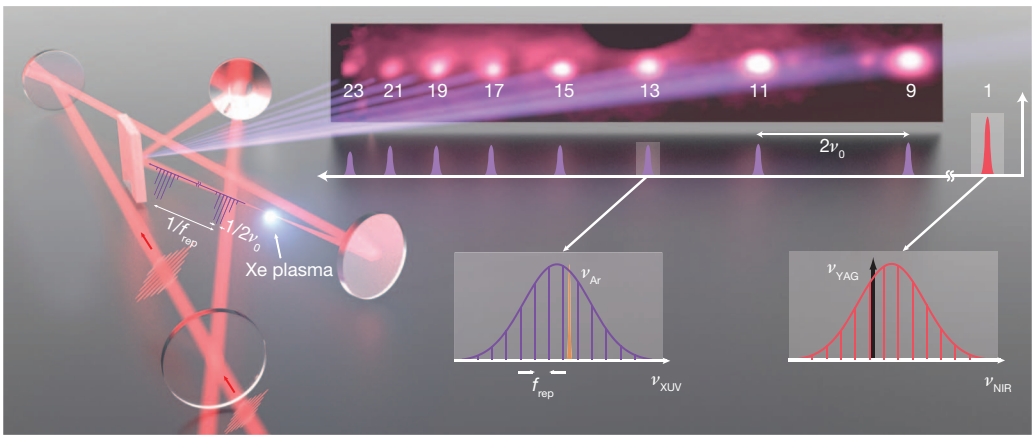

Figure 1 | Intracavity high-harmonic generation. An infrared frequency comb is passively amplified in a power build-up cavity with a mirror/diffraction grating hybrid output coupler for the XUV range[26]. Xenon gas is introduced at the tight focus of the cavity. The resultant HHG spectrum (top inset) from a single infrared pulse consists of odd harmonics of the infrared carrier frequency, ν_0. By using an infinite train of pulses, we create a new comb structure in every harmonic at the repetition frequency (f_{rep}) of the pulse train (lower insets). This comb structure is stabilized using a continuous-wave laser (frequency, ν_{YAG}) and slowly scanned over an argon transition (frequency, ν_{Ar}) at 82 nm. ν_{XUV} and ν_{NIR} respectively represent frequencies in the XUV and near-infrared spectral regions.

[1]JILA, National Institute of Standards and Technology and University of Colorado, Department of Physics, University of Colorado, Boulder, Colorado 80309-0440, USA. [2]IMRA America Inc., 1044 Woodridge Avenue, Ann Arbor, Michigan 48105, USA. †Present address: Institute for Lasers, Life and Biophotonics, Vrije Universiteit Amsterdam, De Boelelaan 1081, 1081HV Amsterdam, The Netherlands.
*These authors contributed equally to this work.

requirements are more stringent for XUV comb generation, where the phase coherence must be maintained over many consecutive pulses. This issue has been a topic of investigation since the first demonstrations of intracavity HHG[3,4], in which only the phase coherence of the third harmonic was verified. In subsequent work, pulse-to-pulse temporal coherence of the seventh harmonic at 152 nm, below the ionization threshold, was demonstrated interferometrically[18]. The pulse-to-pulse phase coherence of above-threshold harmonics in the XUV range was first demonstrated in ref. 8. This coherence was critical for two-pulse Ramsey spectroscopy of helium at 51 nm with a systematic uncertainty of 6 MHz (ref. 8) in a widely tunable system[19]. We note that this approach differs fundamentally from the work presented here. The two-pulse Ramsey sequence is a phase measurement and, as a result, is susceptible to systematic phase errors between the two pulses. These errors lead to apparent frequency shifts. Thus, all sources of phase error must be considered and characterized before an absolute frequency measurement can be made. By contrast, a frequency comb consisting of an infinite pulse train is an optical frequency synthesizer with equally spaced frequency comb teeth, defined by only two numbers: the repetition frequency (f_{rep}) of the pulse train and the carrier envelope offset frequency (f_{ceo}). Thus, the phase instabilities can lead to broadening of the comb teeth, but the absolute frequencies of the XUV comb remain simply and robustly determined. It is precisely this characteristic that led to the recent frequency comb revolution in metrology even though multipulse Ramsey spectroscopy in the visible and infrared spectral regions has existed since the late 1970s[20]. In this Letter, we demonstrate the extension of frequency comb spectroscopy to the XUV spectral region, which will lead to many applications in short-wavelength metrology.

In intracavity HHG, a high-average-power infrared frequency comb[5] is coupled to a dispersion-controlled optical cavity (Fig. 1), which allows for passive coherent pulse build-up at the full repetition rate of 154 MHz (Supplementary Information). The high repetition rate of intracavity HHG should in principle provide increased average flux relative to conventional single-pass HHG systems, which typically use lasers with repetition frequencies and average powers that are smaller by orders of magnitude. However, until now the presence of the optical cavity has presented challenges to matching the average flux of these systems, owing to optical damage problems associated with the large average intracavity power and to the nonlinear-response of the HHG medium. At the high intensities and gas densities required to optimize the XUV flux, the plasma density at the intracavity focus reaches levels that can lead to various nonlinearities such as optical bistability, self-phase modulation and pulse distortion. Recently, these effects have been studied in detail with both simulations and experiments[21,22]. These effects, amplified by the narrow cavity linewidth, clamp the achievable intracavity peak power and lead to instabilities in the lock between the comb and the cavity, limiting the attainable XUV flux and coherence time. Thus, a robust means of mitigating these effects is to decrease the finesse. However, this requires that a more powerful laser be used to excite the enhancement cavity to keep the intracavity pulse energy high. This obstacle has been overcome by recent advances in high-repetition-rate, high-average-power chirped-pulse amplified Yb:fibre lasers[5,23–25].

Our ability to reach high intracavity pulse energies while minimizing the deleterious effects of a large plasma density has resulted in the generation of unprecedented power in high harmonics spectrally separated for spectroscopy. We measure the power in the fifteenth harmonic to be 21 μW with xenon as the target gas (Fig. 2), which corresponds to more than 200 μW per harmonic produced in the cavity. This is an increase of more than an order of magnitude over previous intracavity HHG results[26,27]. Similar outcoupled power (not spectrally separated) was recently reported[28]. We have also observed shorter-wavelength radiation by using krypton as the target gas for HHG. Owing to the higher ionization potential of krypton, we were able to detect the twenty-fifth and twenty-seventh harmonic orders

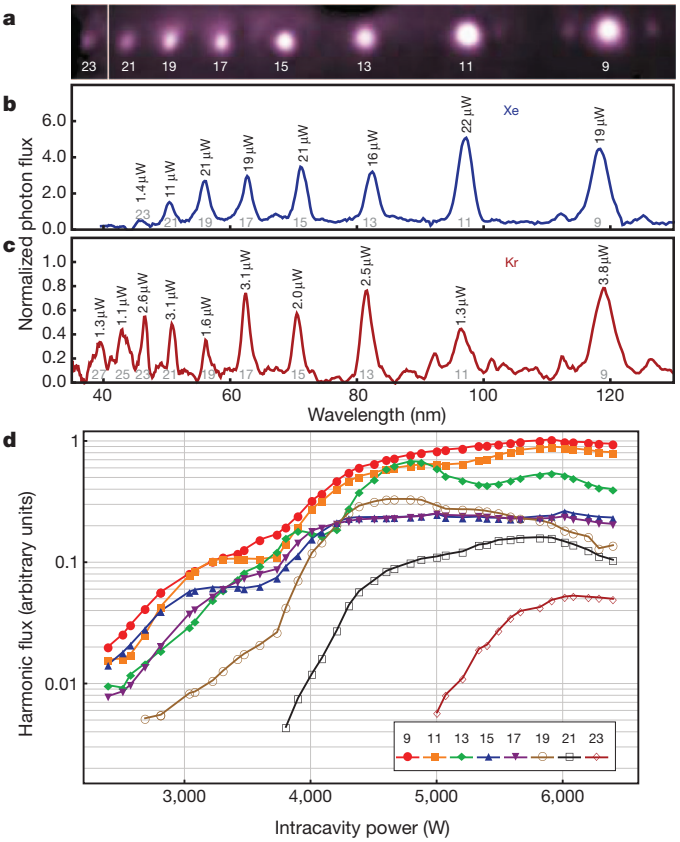

Figure 2 | Power scaling results. **a**, Characteristic image of the harmonics in xenon dispersed on a plate coated with fluorescent material. The threshold of the image was adjusted for the twenty-third harmonic to make it more visible. **b**, **c**, Vertically integrated intensity from a charge-coupled-device (CCD) image for xenon (**b**) and krypton (**c**) target gas, and corresponding integrated harmonic powers (Methods Summary). The observed widths of the harmonic orders are given by the instrument wavelength resolution. The photon flux has been normalized by the spectral bandwidth. **d**, Harmonic powers generated in xenon as functions of infrared intracavity power, showing saturation at powers greater than 5.5 kW. The oscillations visible for some harmonics are due to quantum path interference[18].

with 8 kW of intracavity power (peak intensity of 9×10^{13} W cm^{-2}) (Fig. 2c), extending intracavity HHG to photon energies above 30 eV. As shown in Fig. 2d, there are only modest improvements in power for most harmonics as the intracavity infrared power is increased above 5.5 kW. As the plasma density increases, depletion of the on-axis neutral atomic density and a decrease in phase matching cause the XUV power clamp. These results show that future gains in harmonic power in a similar system will most probably be achieved by increasing the focal area at the interaction region.

To demonstrate the comb structure of XUV radiation, we have spectrally resolved the $3s^2 3p^6\ J = 0 \rightarrow 3s^2 3p^5 5d\ J = 1$ electric dipole (E1) transition in argon with an upper-state energy of 121,932.8 cm^{-1} (corresponding to a wavelength of ~82 nm) and the $2s^2 2p^6\ J = 0 \rightarrow 2s^2 2p^5 4s\ J = 1$ E1 transition in neon with an upper-state energy of 159,534.6 cm^{-1} (~63 nm) by means of resonance fluorescence spectroscopy. These transitions lie within the thirteenth and seventeenth harmonic bandwidths of our source, respectively. To reduce the Doppler width of the transition below the repetition frequency of the comb, we use pulsed supersonic atomic beams propagating orthogonally to the XUV beam. The average harmonic power available for spectroscopy is ~1 μW owing to a single reflection from a mirror to steer the XUV beam into the interaction region and several pinholes to isolate the central part of the beam that contains the phase-coherent short trajectories[18]. Moreover, owing to the electric dipole nature of these transitions, only a single comb tooth with ~10^{-5} of the total power,

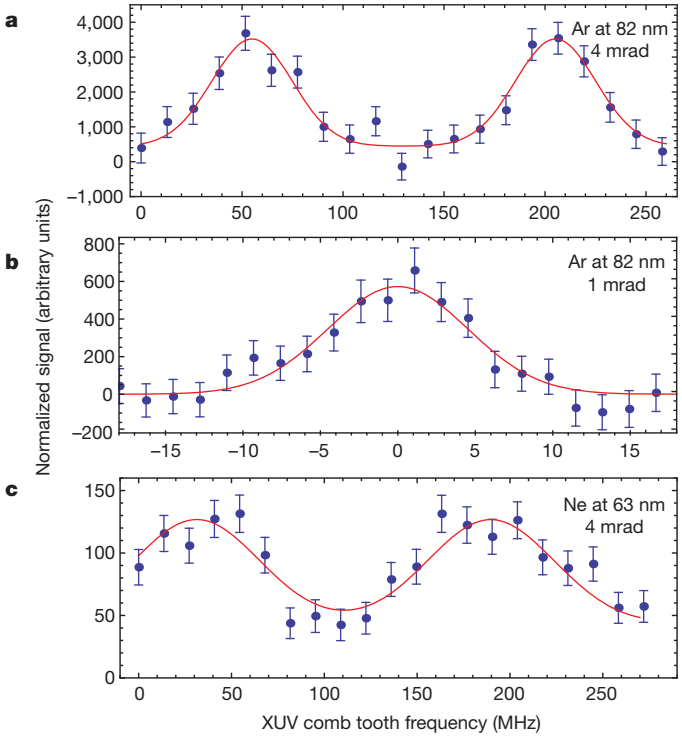

Figure 3 | Atomic fluorescence signal. **a**, **b**, Photomultiplier signals as functions of an XUV comb tooth frequency for argon beam collimation angles of ~4 mrad (**a**) and ~1 mrad (**b**). The signal is normalized to the incident XUV power and the scattered photon background is subtracted (Methods Summary). Error bars (1 s.d.) are determined from the shot noise of counted fluorescence photons. The red curves are least-squares fits to a Gaussian model. **c**, Signal for the neon transition with a collimation angle of ~4 mrad. The contrast and signal-to-noise ratio are lower owing to the increased Doppler width and the smaller absorption cross-section, respectively.

10 pW, contributes to the signal. Nevertheless, we have achieved a ratio of signal to scattered photon background in the range of 0.5–1 using a photomultiplier tube to detect directly the XUV spontaneous emission to the ground state.

The fundamental infrared comb is controlled by phase-locking a comb tooth to a continuous-wave neodymium-doped yttrium aluminium garnet (Nd:YAG) laser by feedback onto the laser cavity length[2]. The Nd:YAG laser frequency (ν_{YAG}) is referenced to a molecular iodine transition and serves as an absolute optical frequency marker with an uncertainty of 5 kHz (ref. 29). The comb offset frequency, f_{ceo}, has a free-running linewidth of 15 kHz (ref. 5) and is adjusted to optimize intracavity power, but is otherwise unlocked. Its value is deduced from the knowledge of ν_{YAG} and f_{rep}, which we measure against the hydrogen maser at the US National Institute of Standards and Technology (Supplementary Information). Figure 3 shows the fluorescence signal as the phase-locked-loop offset frequency, δ, is slowly changed and XUV comb teeth are scanned across the atomic resonance for two different collimation angles of the atomic beam. With the scattered photon background subtracted, the signal contrast is 100%, confirming the sharp comb structure. Least-squares fits for the argon data reveal respective Gaussian full-widths at half-maximum of 47 ± 5 and 11 ± 1 MHz for the two angles. These results are consistent with what would be expected from the geometric collimation. Thus, the observed linewidth places only an upper bound on the comb teeth linewidth, and this bound is less than 10 MHz. The statistical uncertainty in the determination of the line centre for the narrower line shape is 500 kHz, demonstrating an unprecedented fractional frequency precision of better than 2×10^{-10} in the XUV range.

To determine the absolute frequency of the argon transition, it is necessary to determine the comb tooth number in addition to f_{rep} and f_{ceo}. This requires making several measurements at different values of f_{rep} and keeping track of the change in the comb tooth number (Supplementary Information). Figure 4 shows the results of ten measurements at different values of f_{rep} chosen to provide absolute comb mode determination. The data analysis is carried out by noting that the fixed point of the infrared comb (comb tooth phase locked to the Nd:YAG laser) is multiplied by the HHG process to create corresponding fixed points for every harmonic comb. These fixed points are offset from $q\nu_{YAG}$ by $\Delta = q\delta$(modulo f_{rep}), where q is the harmonic order. Thus, the argon transition frequency is

$$\nu_{Ar} = nf_{rep} + 13f_{ceo} = mf_{rep} + 13\nu_{YAG} + \Delta$$

where n is the absolute comb tooth number and m is the difference in comb tooth number between the thirteenth harmonic fixed point and the actual comb tooth probing the argon transition. This point of view not only makes the analysis independent of drifts in f_{ceo}, but also highlights the direct frequency link between the infrared and the higher-harmonic combs.

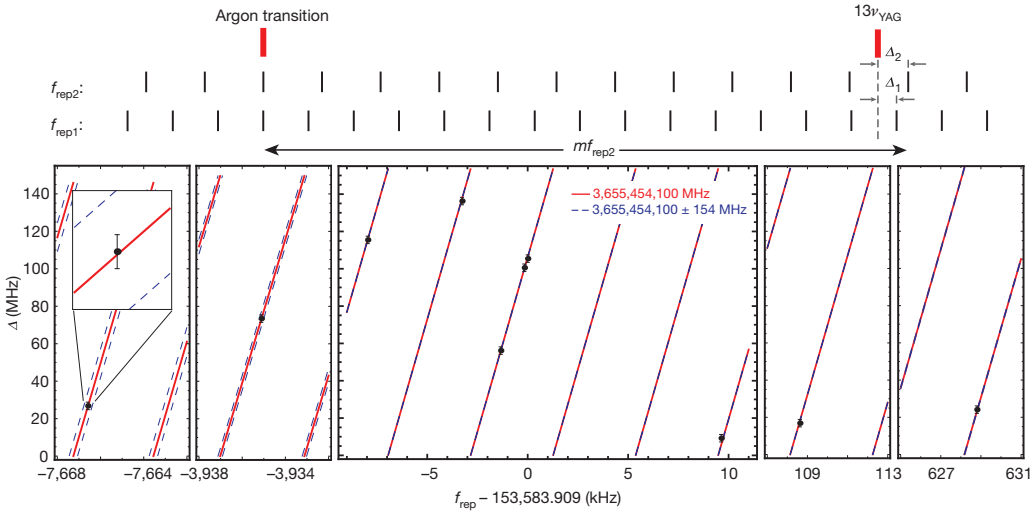

Figure 4 | Absolute frequency determination. Measurement of the resonance centre frequency at ten different values of f_{rep} parameterized by the offset, Δ, of the thirteenth harmonic fixed point from $13\nu_{YAG}$. The top part of the figure schematically illustrates two different measurements at f_{rep1} and f_{rep2}, with corresponding respective offsets of Δ_1 and Δ_2. The short black lines represent the locations of individual frequency comb teeth. In the main plot, the solid red lines show the expected locations of the resonance centres for the extracted comb tooth number, m, and the pairs of blue dashed lines show the expected locations for $m \pm 1$. Inset, magnified version of a measurement, demonstrating that the comb tooth number is unambiguously determined.

Once m is determined, we correct the final value for residual Doppler shifts arising from imperfect orthogonal alignment of the laser and the atomic beam. This is done by comparing the measured transition frequency of a pure argon beam (velocity of $520 \pm 20\ \mathrm{m\,s^{-1}}$) with that of a helium–argon mixture (5:1 ratio of partial pressures; velocity of $740 \pm 60\ \mathrm{m\,s^{-1}}$) and translating the collimation slit until the two measured frequencies match, ensuring orthogonality between the laser and the atomic beams. Owing to the small fractional change in the velocity of the two beams, the uncertainty in the procedure is ~3 MHz. All other systematic shifts such as recoil, density and Stark shifts, as well as the contribution due to the uncertainty in ν_{YAG}, are estimated to be smaller than 1 MHz. We have also binned our data for different laser operation conditions and find no systematic shifts at the 2-MHz level for a 30% change in xenon backing pressure or a 20% change in the intracavity power for HHG, again highlighting the robustness of the XUV comb for frequency measurements. The final absolute frequency for this transition is 3,655,454,073 ± 3 MHz, which agrees well with previous measurements that have an uncertainty of 2.3 GHz (ref. 30).

Now that the XUV frequency comb has been developed into a robust tool, it is imperative to determine its ultimate coherence. The current upper bound on the thirteenth harmonic comb linewidth is less than 10 MHz, limited by the atomic thermal motion. We plan to implement a heterodyne beat measurement between two intracavity HHG sources to overcome this limitation, improving the phase noise characterization by orders of magnitude. With these developments, ultrahigh-precision spectroscopy in the XUV range is firmly within our grasp, enabling a wide range of applications.

METHODS SUMMARY

The Yb:fibre comb delivers 120-fs pulses at a 154-MHz repetition frequency with a maximum average power of 80 W (ref. 5). For the studies presented here, we run the laser at ~30 W. Target gas is injected at the intracavity focus using a glass nozzle with a 100-μm aperture and a backing pressure of ~2 atm. The XUV light is coupled out of the cavity using an intracavity diffraction grating with 10% efficiency[26].

The power of the thirteenth harmonic is measured with an XUV photodiode. The power in the other harmonics is determined using a plate coated with sodium salicylate, which fluoresces at 420 nm when excited by XUV radiation, with uniform quantum efficiency between 40 and 100 nm (ref. 18). The fluorescence is imaged using a CCD camera and calibrated using the thirteenth harmonic, which can be measured with either the photodiode or the CCD. The estimated calibration uncertainty is 20–30%.

The supersonic argon source consists of a pulsed valve nozzle (0.5-mm diameter), a 0.5-mm-diameter skimmer and a secondary slit located 33 cm from the skimmer. Both the slit width and slit position can be adjusted to study the Doppler width and shifts. The valve generates 500-μs-long pulses at a repetition rate of 20 Hz with a backing pressure of 0.5 atm.

The fluorescence is detected with a photomultiplier tube and pulse counter. The counter has two gates: one coincident with the argon pulse arrival time, to measure the signal; and another located between argon pulses, to measure the background. Most of the laser light passes through the interaction region unimpeded and is detected with a second XUV photodiode, which provides the normalization signal. Individual frequency scans take ~150 s. Results presented in Fig. 3 are averages of 3–10 scans with an acquisition time of 8–25 min.

Received 9 September; accepted 3 November 2011.

1. Udem, T., Holzwarth, R. & Hänsch, T. W. Optical frequency metrology. *Nature* **416,** 233–237 (2002).
2. Cundiff, S. T. & Ye, J. Femtosecond optical frequency combs. *Rev. Mod. Phys.* **75,** 325–342 (2003).
3. Jones, R. J., Moll, K. D., Thorpe, M. J. & Ye, J. Phase-coherent frequency combs in the vacuum ultraviolet via high-harmonic generation inside a femtosecond enhancement cavity. *Phys. Rev. Lett.* **94,** 193201 (2005).
4. Gohle, C. *et al.* A frequency comb in the extreme ultraviolet. *Nature* **436,** 234–237 (2005).
5. Ruehl, A., Marcinkevicius, A., Fermann, M. E. & Hartl, I. 80 W, 120 fs Yb-fiber frequency comb. *Opt. Lett.* **35,** 3015–3017 (2010).
6. Merkt, F. & Softley, T. P. Final-state interactions in the zero-kinetic-energy-photoelectron spectrum of H_2. *J. Chem. Phys.* **96,** 4149–4156 (1992).
7. Herrmann, M. *et al.* Feasibility of coherent XUV spectroscopy on the 1S–2S transition in singly ionized helium. *Phys. Rev. A* **79,** 052505 (2009).
8. Kandula, D. Z., Gohle, C., Pinkert, T. J., Ubachs, W. & Eikema, K. S. E. Extreme ultraviolet frequency comb metrology. *Phys. Rev. Lett.* **105,** 063001 (2010).
9. Eyler, E. E. *et al.* Prospects for precision measurements of atomic helium using direct frequency comb spectroscopy. *Eur. Phys. J. D* **48,** 43–55 (2008).
10. Peik, E. & Tamm, C. Nuclear laser spectroscopy of the 3.5 eV transition in Th-229. *Europhys. Lett.* **61,** 181–186 (2003).
11. Rellergert, W. G. *et al.* Constraining the evolution of the fundamental constants with a solid-state optical frequency reference based on the ^{229}Th nucleus. *Phys. Rev. Lett.* **104,** 200802 (2010).
12. Campbell, C. J., Radnaev, A. G. & Kuzmich, A. Wigner crystals of ^{229}Th for optical excitation of the nuclear isomer. *Phys. Rev. Lett.* **106,** 223001 (2011).
13. Murphy, M. T., Webb, J. K. & Flambaum, V. V. Further evidence for a variable fine-structure constant from Keck/HIRES QSO absorption spectra. *Mon. Not. R. Astron. Soc.* **345,** 609–638 (2003).
14. Berengut, J. C., Dzuba, V. A., Flambaum, V. V. & Ong, A. Electron-hole transitions in multiply charged ions for precision laser spectroscopy and searching for variations in alpha. *Phys. Rev. Lett.* **106,** 210802 (2011).
15. Krausz, F. & Ivanov, M. Attosecond physics. *Rev. Mod. Phys.* **81,** 163–234 (2009).
16. Bellini, M. *et al.* Temporal coherence of ultrashort high-order harmonic pulses. *Phys. Rev. Lett.* **81,** 297–300 (1998).
17. Mairesse, Y. *et al.* Attosecond synchronization of high-harmonic soft X-rays. *Science* **302,** 1540–1543 (2003).
18. Yost, D. C. *et al.* Vacuum-ultraviolet frequency combs from below-threshold harmonics. *Nature Phys.* **5,** 815–820 (2009).
19. Pinkert, T. J. *et al.* Widely tunable extreme UV frequency comb generation. *Opt. Lett.* **36,** 2026–2028 (2011).
20. Eckstein, J. N., Ferguson, A. I. & Hänsch, T. W. High-resolution two-photon spectroscopy with picosecond light pulses. *Phys. Rev. Lett.* **40,** 847–850 (1978).
21. Allison, T. K., Cingöz, A., Yost, D. C. & Ye, J. Extreme nonlinear optics in a femtosecond enhancement cavity. *Phys. Rev. Lett.* **107,** 183903 (2011).
22. Carlson, D. R., Lee, J., Mongelli, J., Wright, E. M. & Jones, R. J. Intracavity ionization and pulse formation in femtosecond enhancement cavities. *Opt. Lett.* **36,** 2991–2993 (2011).
23. Hartl, I. *et al.* Cavity-enhanced similariton Yb-fiber laser frequency comb: 3×10^{14} W/cm^2 peak intensity at 136 MHz. *Opt. Lett.* **32,** 2870–2872 (2007).
24. Schibli, T. R. *et al.* Optical frequency comb with submillihertz linewidth and more than 10 W average power. *Nature Photon.* **2,** 355–359 (2008).
25. Eidam, T. *et al.* Femtosecond fiber CPA system emitting 830 W average output power. *Opt. Lett.* **35,** 94–96 (2010).
26. Yost, D. C., Schibli, T. R. & Ye, J. Efficient output coupling of intracavity high-harmonic generation. *Opt. Lett.* **33,** 1099–1101 (2008).
27. Ozawa, A. *et al.* High harmonic frequency combs for high resolution spectroscopy. *Phys. Rev. Lett.* **100,** 253901 (2008).
28. Lee, J., Carlson, D. & Jones, R. J. Optimizing intracavity high harmonic generation for XUV fs frequency combs. *Opt. Express* **19,** 23315–23326 (2011).
29. Ye, J., Ma, L.-S. & Hall, J. L. Molecular iodine clock. *Phys. Rev. Lett.* **87,** 270801 (2001).
30. Minnhagen, L. Spectrum and the energy levels of neutral argon, Ar I. *J. Opt. Soc. Am.* **63,** 1185–1198 (1973).

Supplementary Information is linked to the online version of the paper at www.nature.com/nature.

Acknowledgements We thank J. L. Hall for the use of an iodine-stabilized laser, M. D. Swallows for the assistance with the hydrogen maser frequency transfer, and S. T. Cundiff and A. Foltynowicz for reading a draft of the manuscript. This research is funded by the DARPA, AFOSR, NIST and NSF. A.C. and T.K.A. are National Research Council postdoctoral fellows. A.R. acknowledges funding from the Alexander von Humboldt Foundation (Germany).

Author Contributions A.C., D.C.Y., T.K.A. and J.Y. conceived of, designed and carried out the XUV power and spectroscopy measurements. A.R., M.E.F. and I.H. designed and built the Yb:fibre laser. All authors discussed the results and worked on the manuscript.

Author Information Reprints and permissions information is available at www.nature.com/reprints. The authors declare no competing financial interests. Readers are welcome to comment on the online version of this article at www.nature.com/nature. Correspondence and requests for materials should be addressed to A.C. (acingoz@jila.colorado.edu) or J.Y. (junye@jila.colorado.edu).